



Swansea University
Prifysgol Abertawe



Cronfa - Swansea University Open Access Repository

This is an author produced version of a paper published in:

Hyperfine Interactions

Cronfa URL for this paper:

<http://cronfa.swan.ac.uk/Record/cronfa44932>

Paper:

Kadyrov, A., Rawlins, C., Charlton, M., Fabrikant, I. & Bray, I. (2018). Antihydrogen formation in low-energy antiproton collisions with excited-state positronium atoms. *Hyperfine Interactions*, 239(1)

<http://dx.doi.org/10.1007/s10751-018-1519-x>

This item is brought to you by Swansea University. Any person downloading material is agreeing to abide by the terms of the repository licence. Copies of full text items may be used or reproduced in any format or medium, without prior permission for personal research or study, educational or non-commercial purposes only. The copyright for any work remains with the original author unless otherwise specified. The full-text must not be sold in any format or medium without the formal permission of the copyright holder.

Permission for multiple reproductions should be obtained from the original author.

Authors are personally responsible for adhering to copyright and publisher restrictions when uploading content to the repository.

<http://www.swansea.ac.uk/library/researchsupport/ris-support/>

Antihydrogen formation in low-energy antiproton collisions with excited-state positronium atoms

A. S. Kadyrov · C. M. Rawlins ·
M. Charlton · I. I. Fabrikant · I. Bray

Received: date / Accepted: date

Abstract The convergent close-coupling method is used to obtain cross sections for antihydrogen formation in low-energy antiproton collisions with positronium (Ps) atoms in specified initial excited states with principal quantum numbers $n_i \leq 5$. The threshold behaviour as a function of the Ps kinetic energy, E , is consistent with the $1/E$ law expected from threshold theory for all initial states. We find that the increase in the cross sections is muted above $n_i = 3$ and that here their scaling is roughly consistent with n_i^2 , rather than the classically expected increase as n_i^4 .

Keywords Antihydrogen · Antiproton · Positronium

PACS 34.80.-i

1 Introduction

Physics with antihydrogen ($\bar{\text{H}}$) at low energies has made great progress recently (see [1] for a review) whereby trapped samples of the antiatoms [2, 3] have been used to make measurements of some its properties [4, 5], including landmark observations of the 1s-2s two photon transition [6] and features of the ground state hyperfine spectrum [7].

A. S. Kadyrov · C. M. Rawlins · I. Bray
Curtin Institute for Computation and Department of Physics and Astronomy, Curtin University, GPO Box U1987, Perth, WA 6845, Australia

M. Charlton
Department of Physics, College of Science, Swansea University, Swansea SA2 8PP, UK

I. I. Fabrikant
Department of Physics and Astronomy, University of Nebraska, Lincoln, Nebraska 68588-0299, USA

These experiments were performed by creating $\bar{\text{H}}$ via the three-body positron (e^+) antiproton (\bar{p}) reaction $e^+ + e^+ + \bar{p} \rightarrow \bar{\text{H}} + e^+$ [8,9]. It is well known (see [10] and references therein) that this reaction produces $\bar{\text{H}}$ in highly excited states (typical binding energies are of order of a few $k_B T_e$, with k_B Boltzmann's constant, and T_e the positron temperature) such that trapping is mandatory for experimentation on the ground (1s) state. Furthermore, to promote both the rate of reaction, and the probability of trapping, both T_e and the \bar{p} equivalent should be as low as possible. To give some context, the state-of-the-art magnetic minimum $\bar{\text{H}}$ trap employed by the ALPHA collaboration is only around 0.54 K deep [11], and given the technical challenges associated with such devices, it is unlikely that trap depths significantly greater than this will be available in the near future.

Currently, ALPHA's experiments [3] form $\bar{\text{H}}$ via $e^+ - \bar{p}$ mixing with $T_e \sim 20$ K such that the trapped anti-atoms originate from the tail of a thermal distribution [2], resulting in capture efficiencies of order 10^{-4} of the total $\bar{\text{H}}$ yield. Increasing the trapping efficiency (using the $e^+ - \bar{p}$ scheme) only seems feasible via reductions in T_e , and there is ongoing effort to reach the few K temperature region, as discussed in [12]. The $e^+ - \bar{p}$ scheme demands that the mixing procedure does not markedly increase T_e , and that the \bar{p} temperature, which governs that of the $\bar{\text{H}}$, is determined by (and is as close to as possible) T_e . Thus, both species must be as cold to enhance the probability of forming trappable antihydrogen.

An alternative to $e^+ + e^+ + \bar{p} \rightarrow \bar{\text{H}} + e^+$ is the reaction

$$\text{Ps}(n_i, l_i) + \bar{p} \rightarrow \bar{\text{H}}(n', l') + e^-, \quad (1)$$

as suggested some time ago [13–15]. Here the colliding Ps state is characterised by n_i and l_i , the principal and orbital angular momentum quantum numbers respectively, with n' and l' being the corresponding values for $\bar{\text{H}}$. This reaction was observed in a demonstration experiment [16] using a double charge exchange scheme [17], and the ATRAP collaboration is making preparations for further work in this respect [18]. The AEGIS [19,20] and GBAR [21,22] collaborations plan to exploit reaction (1) to form beams of $\bar{\text{H}}$ for studies of antimatter gravity. In both cases laser-excited Ps will be used as the scattering target, and in particular AEGIS plans to use highly excited states interacting with cold \bar{p} to form $\bar{\text{H}}$ capable of Stark acceleration (see e.g. [23]) into a beam for deflectometry studies. That experiment will exploit one of the potential advantages of reaction (1), namely that low-energy (see below) excited-state Ps reacting with an effectively stationary, trapped \bar{p} will impart little momentum in the collision, thereby reducing heating. As such, cold (and possibly trappable) $\bar{\text{H}}$ can be produced, requiring that only the \bar{p} (and not both antiparticle species) are cold before the interaction.

Despite the long term interest in reaction (1) (and its charge-conjugate time-reverse, Ps formation in $e^+ - \text{H}$ collisions), it is only recently that reliable values for the cross sections for this process, $\sigma_{\bar{\text{H}}}$, have been available for excited states of Ps, and at the low (sub-eV) energies of current interest [24–27]. These studies have involved the application of Convergent Close Coupling (CCC)

and Threshold Theory (TT) approaches, and further details of these will be provided in section 2.

The initial excited-state Ps work [24,25] found large enhancements in $\sigma_{\bar{H}}$ for the $n_i = 2$ and 3 states (e.g., around factors of 50 for $n_i = 1-2$ and 25 for $n_i = 2-3$ at 0.1 eV), with excellent agreement evident between the $n_i = 1$ CCC data and the essentially exact variational results of Humberston and co-workers [28]. Furthermore, the cross sections for the excited states were found to vary as $1/E$, with E the Ps kinetic energy, in the energy range below about 1 eV, which is of relevance given typical emission energies from current vacuum sources of Ps (see e.g., [29,30]).

Very recently [27], the CCC and TT calculations were extended to $n_i = 4$ and 5, and, surprisingly, the increases in $\sigma_{\bar{H}}$ were found to be much muted in comparison to the lower states, with the variation found to be close to a scaling of n_i^2 , rather than the n_i^4 law expected from a Bohr-type analysis. This phenomenon was attributed to the suppression of higher angular momentum contributions to the cross section, as described briefly in section 2 and in more detail in [27].

In [27], emphasis was placed upon the implications of the discovery of the quantum suppression effect, and this was best illustrated by presenting cross section data summed at each n_i across the Ps l_i manifold. Of most experimental interest, however, are cross sections resolved by Ps state (see the discussion in section 3), and we present these data here. The remainder of this article is organised as follows. Section 2 contains descriptions of the CCC and TT approaches used to derive values for $\sigma_{\bar{H}}$ at low Ps energies, the main results are presented in section 3 and conclusions are drawn in section 4.

2 Theoretical Details

Originally, the CCC method was developed for positron scattering on H [31, 32]. Later it was extended to positron scattering on multi-electron targets (see, e.g. [33,34]). In positron scattering the primary challenge is to account for Ps-formation channels. The CCC approach combines the expansion of the total wave function over the target states with the expansion over the Ps states, therefore it allows for explicit Ps formation. The two-centre CCC formalism for positron-hydrogen scattering was used to calculate cross sections for Ps formation [32], and thereby those for the reverse process of Ps scattering on a proton to yield hydrogen formation [35]. By symmetry, this is equivalent to Ps scattering on an antiproton leading to the formation of antihydrogen. Comprehensive details of the formalism have been given by Kadyrov and Bray [32], who have also provided a recent review of applications of the CCC theory to positron-atom scattering [36].

Briefly, the calculations used here are the same as those that were recently presented [27], but now given for specific initial Ps states. They were generated by using two separate eigenstate expansions on H with $n' \leq 7$ and Ps with $n_i \leq 5$ ($0 \leq l_i \leq n_i - 1$). For this reason we are able to provide cross sections

for $\text{Ps}(n_i, l_i)$ individual initial states scattering with antiprotons to form anti-hydrogen for $n' \leq 7$, which we present as summed over all open final states. The intention here is to provide the data that are of relevance to experiments interested in laser-excitation of Ps prior to collisions with antiprotons.

The low-energy and threshold behaviour of cross sections for collisions of Ps with antiprotons is controlled by the long-range interaction. If the Ps is in its ground state, the dominant interaction is due to polarisation, which decays as $1/r^4$ at large distances. According to the Wigner threshold law [37], in this case the elastic cross section is finite at zero energy, and the cross sections for endothermic processes behave as $(E - E_t)^{l_{\min}+1/2}$ where E_t is the threshold energy, and l_{\min} is the lowest angular momentum of the projectile relative to the target allowed by symmetry. Accordingly, the cross section for an exothermic reaction varies at low energies as $E^{l_{\min}-1/2}$.

However, if the Ps is in an excited state the dominant Ps- \bar{p} long-range potential is dipolar, which decays as $1/r^2$. This occurs because degenerate states belonging to an l_i manifold (at a given n_i) are dipole coupled due to the presence of an external charge. The theory of the threshold behaviour of elastic and inelastic collision cross sections controlled by such an interaction was developed by Gailitis and Damburg [38, 39]. For each partial wave characterised by the total angular momentum L and parity P , the threshold behaviour is determined by the competition between the attractive dipolar interaction and a repulsive centrifugal barrier. If, for a given L and P , the attractive dipole interaction dominates, the partial cross section for an endothermic reaction is finite at the threshold, and the cross section for an exothermic reaction diverges as $1/E$. Furthermore, elastic and l_i -mixing cross sections exhibit pronounced oscillations at low energies which are best visible when plotted as a function of $\log E$ and, below inelastic thresholds, all cross sections exhibit resonances due to dipole-supported quasi-bound states. However, if the centrifugal barrier dominates, the cross sections for exothermic reactions approach zero as E^a , where the threshold exponent a depends on L , P and the long-range coupling between the degenerate channels. These two regimes are separated by the boundary value L_b of the total angular momentum L [27]. Calculations of Ps- \bar{p} cross sections incorporating these features were accomplished in Refs. [40, 41].

This behaviour is different from that observed in a classical treatment of collisions. For example, in the case of an endothermic reaction controlled by a short-range interaction the Wigner law predicts an $(E - E_t)^{1/2}$ behaviour, whereas according to classical mechanics the cross section should be finite at the threshold. This phenomenon was dubbed “quantum suppression” [42]. Another example of quantum suppression is elastic scattering by a potential which decays faster than $1/r^3$ at large distances. In quantum mechanics the scattering cross section in this case is finite, whereas in classical mechanics it is infinite unless the potential is identically equal to zero beyond some distance r . Generally quantum effects can lead to both suppression and enhancement, as was analysed in detail in Ref. [41].

We have found a remarkable manifestation of the quantum suppression in reaction (1) [27]. According to classical mechanics this reaction effectively occurs for all impact parameters below the Bohr size of the Ps atom, which is proportional to n_i^2 . Accordingly, the cross section for this reaction is proportional to n_i^4 , as confirmed by Classical Trajectory Monte Carlo (CTMC) calculations [17, 43]. However, in quantum mechanics the situation near threshold is different. The highest angular momentum giving a substantial contribution to the reaction cross section is given by L_b , and this quantity is approximately linearly dependent on n_i . This results in an n_i^2 growth of the cross section, in contrast to the fourth power expected from classical mechanics. This is demonstrated by the CCC calculations [27], as described in section 3.

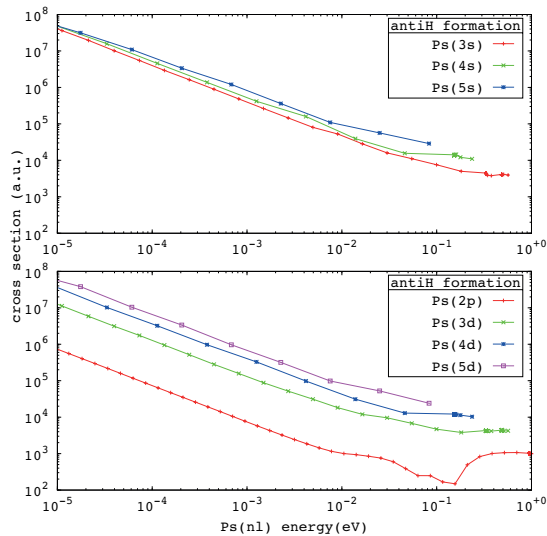


Fig. 1 Cross sections for $\bar{\text{H}}$ formation in \bar{p} -Ps scattering from states accessible by successive single photon excitation interactions from the 1s ground state (see text for details) summed across all $\bar{\text{H}}$ final states.

3 Results and Discussion

From an experimental perspective, the Ps used in reaction (1) is likely to emanate into vacuum from a porous silica sample [29, 30] in the triplet 1s ground state. To promote the rate of $\bar{\text{H}}$ formation excited states will be produced using laser excitation (see e.g., [44–46]) via the 1s-2p single photon transition, or perhaps via the two-photon 1s-2s route. Accordingly, we present the cross sections in three groups: (i) 2p, n_i s and n_i d, as shown in Fig. 1; (ii) 2s, n_i p in Fig. 2 (with the $n_i = 2$ and 3 data from [24, 25] and the $n_i = 4$ and 5 data from the present study in both cases); and (iii) in Fig. 3 the remaining data

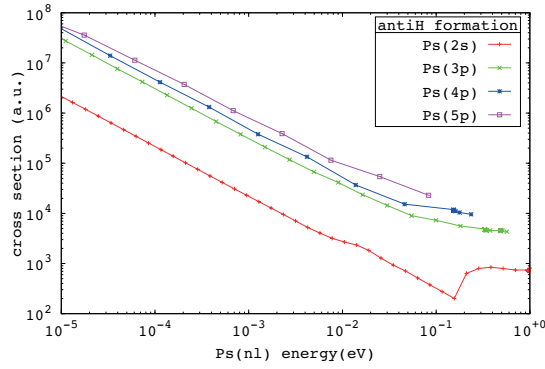


Fig. 2 Cross sections for $\bar{\text{H}}$ formation in \bar{p} -Ps scattering from states accessible following two-photon 1s-2s excitation (see text for details) summed across all $\bar{\text{H}}$ final states.

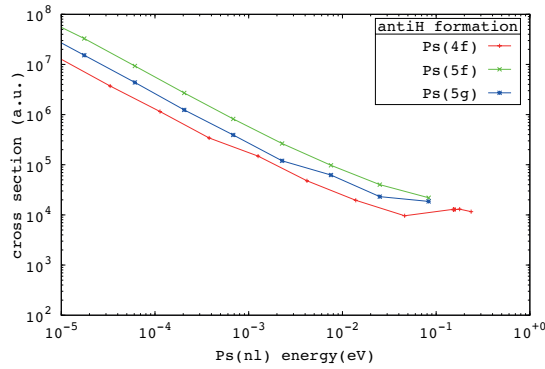


Fig. 3 Cross sections for $\bar{\text{H}}$ formation in \bar{p} -Ps scattering from the remaining states in the $n_{\text{Ps}} = 4$ and 5 manifolds summed across all $\bar{\text{H}}$ final states.

from the $n_i = 4$ and 5 manifolds, namely for the 4f, 5f and 5g Ps states. In each case the cross sections are summed over all final $\bar{\text{H}}$ (n', l') states. Taking the $n_i = 5$ data from Figs. 1-3 at a Ps kinetic energy of 10 meV as an example, the partial cross sections are similar for the different values of l_i at just below 10^5 a.u., though with the 5g results a little lower. A similar effect is present in the $n_i = 4$ data.

All the cross sections shown in Figs. 1-3 exhibit the characteristic $1/E$ behaviour at low energies, in accordance with the threshold law expectations. Regarding their absolute magnitudes, whereas the cross sections enhance substantially when n_i increases from 2 to 3, growth as n_i is raised further is significantly slower, and definitely below the the classical expectation of n_i^4 (see e.g., [17, 43]), and more in accord with the quantum threshold theory prediction of n_i^2 [27]. This is highlighted in Fig. 4 where the cross sections are replotted groups (s, p and d values at the various n_i), scaled by n_i^{-2} . From here the change in the behaviour of the cross section magnitude between $n_i = 2$

and 3 is immediately apparent, along with the n_i^2 scaling, with the latter most closely followed by the data for the s- and p-states.

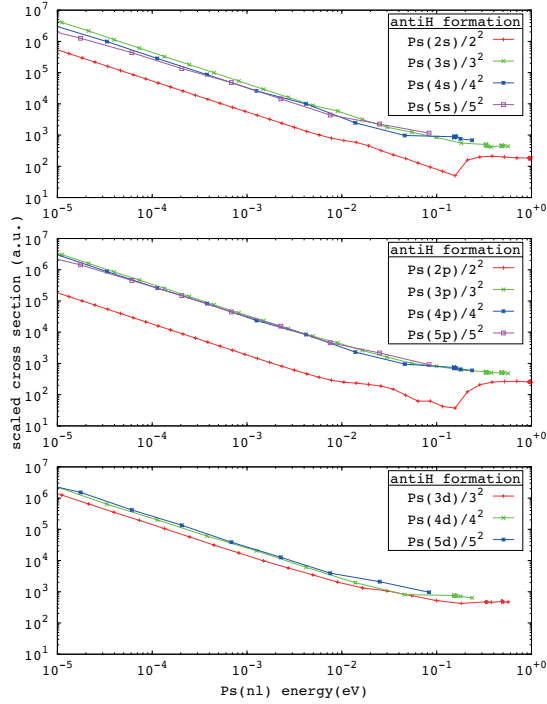


Fig. 4 The cross sections for $\bar{\text{H}}$ formation in \bar{p} -Ps(n_i, l_i) scattering scaled, by n_i^{-2} for $l_i = 0, 1$ and 2.

4 Concluding Remarks

In this paper we have presented the first reliable data for $\sigma_{\bar{\text{H}}}$ for reaction (1) for $n_i = 4$ and 5, disaggregated by the angular momentum state of the colliding Ps. Qualitatively, the expected threshold behaviour of $\sigma_{\bar{\text{H}}} \propto 1/E$ is confirmed for the individual states. Thus, from an experimental perspective, it is desirable to search for efficient sources of Ps at ever lower kinetic energies.

Furthermore, it is notable that the trend of large increases in $\sigma_{\bar{\text{H}}}$ found in [24, 25] across the range $n_i = 1-3$ is not maintained. Indeed, the cross sections, as elucidated in [27], and described briefly in section 2, rise as n_i^2 , which is also depressed in comparison to the n_i^4 classical expectation.

The results are of relevance for $\bar{\text{H}}$ experiments planning to use reaction (1) (e.g., [19–22]), and possibly other applications involving charge exchange in Ps collisions with ionic species [47]. Some of these initiatives intend to use

Rydberg Ps (say species with $n_i = 10$ or above), and the present work must cast doubt on estimates used to assess experimental feasibility. Nevertheless, the expectation is that at sufficiently high principal quantum number, the classical scaling should be appropriate [27], however the absolute cross sections needed by experiment are unknown. Thus, extending studies of reaction (1) to higher n_i using the CCC and TT methods is under consideration.

Acknowledgements The Australian Research Council, the EPSRC (UK) and the US National Science Foundation (via grant No. PHY-1401788) are thanked for their support.

References

1. Bertsche W A, Butler E, Charlton M and Madsen N 2015 *J. Phys. B* **48** 232001
2. Andresen G B *et al.* ALPHA Collaboration 2010 *Nature* **468** 673-6
3. Ahmadi M *et al.* ALPHA Collaboration 2017 *Nature Commun.* **8** 681
4. Amole C *et al.* ALPHA Collaboration 2012 *Nature* **483** 439-43
5. Ahmadi M *et al.* ALPHA Collaboration 2016 *Nature* **529** 373-6
6. Ahmadi M *et al.* ALPHA Collaboration 2017 *Nature* **541** 506-10
7. Ahmadi M *et al.* ALPHA Collaboration 2017 *Nature* **548** 66-70
8. Amoretti M *et al.* ATHENA Collaboration 2002 *Nature* **419** 456-9
9. Gabrielse G *et al.* ATRAP Collaboration 2002 *Phys. Rev. Lett.* **89** 213401
10. Holzscheiter M H, Charlton M and Nieto M M 2004 *Phys. Rep.* **402** 1-101
11. Amole C *et al.* ALPHA Collaboration 2014 *Nucl. Instr. Meth. Phys. Res. A* **735** 319-40
12. Madsen N, Robicheaux F and Jonsell S 2014 *New J. Phys.* **16** 063046
13. Humberston J W, Charlton M, Jacobsen F M and Deutch B I 1987 *J. Phys B* **20** L25-9
14. Charlton M 1990 *Phys. Letts A* **143** 143-6
15. Deutch B I *et al.* 1993 *Hyperfine Interact.* **76** 153-61
16. Storry C H *et al.* ATRAP Collaboration 2004 *Phys. Rev. Lett.* **93** 263401
17. Hessels E A, Homan D M and Cavagnero M J 1998 *Phys. Rev. A* **57** 1668-71
18. McConnell R *et al.* ATRAP Collaboration 2016 *J. Phys. B* **49** 064002
19. Krasnický D *et al.* AEGIS Collaboration 2014 *Int. J. Mod. Phys. Conf. Ser.* **30** 1460262
20. Doser M *et al.* AEGIS Collaboration 2012 *Class. Quant. Grav.* **29** 184009
21. van der Werf D P 2014 *Int. J. Mod. Phys. Conf. Ser.* **30** 1460263
22. Pérez P *et al.* GBAR Collaboration 2015 *Hyperfine Interact.* **233** 21-7
23. Hogan S D 2016 *EPJ Tech.* **3** 2
24. Kadyrov A S *et al.* 2015 *Phys. Rev. Lett.* **114** 183201
25. Rawlins C M *et al.* 2016 *Phys. Rev. A* **93** 012709
26. Charlton M, Kadyrov A S and Bray I and 2016 *Phys. Rev. A* **94** 032701
27. Kadyrov A S, Bray I, Charlton M and Fabrikant I I 2017 *Nature Commun.* **8** 1544
28. Humberston J W *et al.* 1997 *J. Phys. B* **30** 2477-93
29. Crivelli P *et al.* 2010 *Phys. Rev. A* **81** 052705
30. Cassidy D B *et al.* 2010 *Phys. Rev. A* **81** 012715
31. Kadyrov A S and Bray I 2000 *J. Phys. B* **33** L635-L640
32. Kadyrov A S and Bray I 2002 *Phys. Rev. A* **66** 012710
33. Utamuratov R, Kadyrov A S, Fursa D V, and Bray I 2010 *J. Phys. B* **43** 031001
34. Lugovskoy A V, Kadyrov A S, Bray I, and Stelbovics A T 2010 *Phys. Rev. A* **82** 062708
35. Kadyrov A S, Lugovskoy A V, Utamuratov R and Bray I 2013 *Phys. Rev. A* **87** 060701
36. Kadyrov A S and Bray I 2016 *J. Phys. B* **49** 222002
37. Wigner E P 1948 *Phys. Rev.* **73** 1002-9
38. Gailitis M and Damburg R 1963 *Proc. Phys. Soc.* **82** 192-200
39. Gailitis M 1982 *J. Phys. B* **15** 3423-40
40. Fabrikant I I, Bray A, Kadyrov A S and Bray I 2016 *Phys. Rev. A* **94** 012701
41. Fabrikant I I, Kadyrov A S, Bray I, and Charlton M 2017 *J. Phys. B* **50** 134001
42. Côté R, Heller E J, and Dalgarno A 1996 *Phys. Rev. A* **53** 234-41
43. Krasnický D, Caravita R, Canali C, and Testera G 2016 *Phys. Rev. A* **94** 022714
44. Aghion S *et al.* AEGIS Collaboration 2016 *Phys. Rev. A* **94** 102507
45. Jones A C L *et al.* 2017 *J. Phys. B* **49** 064006
46. Baker C J *et al.* 2018 *J. Phys. B* **51** 035006
47. Bertsche W A, Charlton M and Eriksson S 2017 *New J. Phys.* **19** 053020